An observation-based method to assess tropical stratocumulus and shallow cumulus clouds and feedbacks in CMIP6 and CMIP5 models

G. V. Cesana, A. S. Ackerman, N. Črnivec, R. Pincus, H. Chepfer

An observation-based method to assess tropical stratocumulus and shallow cumulus clouds and feedbacks in CMIP6 and CMIP5 models

Environmental Research Communications

PAPER

An observation-based method to assess tropical stratocumulus and shallow cumulus clouds and feedbacks in CMIP6 and CMIP5 models

G V Cesana[1,2,*], **A S Ackerman**[2], **N Črnivec**[1,2], **R Pincus**[3] and **H Chepfer**[4]

[1] Center for Climate Systems Research, Columbia University, NY, United States of America
[2] NASA Goddard Institute for Space Studies, NY, United States of America
[3] Lamont-Doherty Earth Observatory, Columbia University, NY, United States of America
[4] LMD/IPSL, Sorbonne Université, École Polytechnique, CNRS, Paris, France
[*] Author to whom any correspondence should be addressed.

E-mail: gregory.cesana@columbia.edu

OPEN ACCESS

RECEIVED
13 January 2023

REVISED
15 March 2023

ACCEPTED FOR PUBLICATION
24 March 2023

PUBLISHED
5 April 2023

Keywords: stratocumulus, shallow cumulus, low-cloud feedback, CALIPSO-GOCCP, CMIP, climate model evaluation

Supplementary material for this article is available online

Abstract

In the Earth system models (ESMs) participating in the Coupled Models Intercomparison Project phase 6 (CMIP6), the tropical low-cloud feedback is 50% more positive than its predecessors (CMIP5) and continues to dominate the spread in simulated climate sensitivity. In the context of recent studies reporting larger feedbacks for stratocumulus (Sc) than shallow cumulus (Cu) clouds, it appears crucial to faithfully represent the geographical extent of each cloud type to simulate realistic low-cloud feedbacks. Here we use a novel observation-based method to distinguish Sc and Cu clouds together with satellite data from Cloud-Aerosol Lidar and Infrared Pathfinder Satellite Observations (CALIPSO) and Clouds and the Earth's Radiant Energy System (CERES) to evaluate Sc and Cu cloud fractions, cloud radiative effects and cloud feedbacks in the two latest generations of CMIP ESMs. Overall, the CMIP6 models perform better than the CMIP5 models in most aspects considered here, indicating progress. Yet the ensemble mean continues to underestimate the marine tropical low-cloud fraction, mostly attributable to Sc. Decomposition of the bias reveals that the Sc-regime cloud fraction is better represented in CMIP6, although Sc regimes occur too infrequently—even less frequently than in CMIP5. Building on our Sc and Cu discrimination method, we demonstrate that CMIP6 models also simulate more realistic low-cloud feedbacks than CMIP5 models, especially the Sc component. Finally, our results suggest that part of the CMIP6 low-cloud feedback increase can be traced back to greater cloud fraction in Sc-dominated regions.

1. Introduction

How clouds will respond to global warming, which is the essence of cloud feedback, continues to be a leading source of uncertainty in the two most recent Coupled Models Intercomparison Project (CMIP) generations (Zelinka *et al* 2016, 2020). The associated diversity of behavior impedes our ability to project the magnitude of future climate change and associated impacts (Vial *et al* 2013, Caldwell *et al* 2016, Zelinka *et al* 2020). More specifically, tropical low-cloud feedbacks, which are about 50% larger in CMIP6 (Cesana and del Genio 2021), remain particularly challenging because they dominate the spread among Earth system model (ESM) estimates of equilibrium climate sensitivity (ECS), a measure of the globally averaged surface air warming resulting from a doubling of CO_2 (Bony and Dufresne 2005, Andrews *et al* 2012, Vial *et al* 2013, Caldwell *et al* 2016).

Low clouds may be separated into two main categories: stratocumulus (Sc, including stratus clouds), typically driven by cloud-top radiative cooling, and shallow cumulus (Cu), driven by surface heat fluxes. Since these low clouds are dominated by different processes, they are typically represented by different parametrizations (i.e., turbulence for Sc and plume-like convection for Cu), and they exhibit distinct sensitivities to sea surface temperature (SST) and estimated inversion strength ([EIS]; Cesana and del Genio 2021,

Myers *et al* 2021), the two main low-cloud controlling factors (Qu *et al* 2015, Klein *et al* 2017). As a result, Sc and Cu clouds generate distinct feedbacks that are modulated by SST and EIS patterns (e.g., Andrews and Webb 2018, Cesana and del Genio 2021). Consequently, simulating Sc or Cu clouds in the wrong places may result in unrealistic feedbacks, which explains why the issue of the Sc and Cu geographical extent emerges as being essential to estimating low-cloud feedbacks and the contribution to simulated ECS.

However, most past studies have investigated low-cloud feedbacks as a whole rather than separating the contribution of Sc and Cu (Bony and Dufresne 2005, Soden and Held 2006, Zelinka *et al* 2013, 2016). This limitation is partly driven by a lack of observations that distinguish these cloud regimes (mostly field campaigns and ground-based sites, e.g., Rémillard *et al* 2012) and partly because it has been difficult to distinguish them in ESM outputs. The advent of new Sc and Cu global-scale datasets, such as the Cumulus And Stratocumulus CloudSat-CAlipso Dataset (CASCCAD; Cesana *et al* 2019b), provide new possibilities in ESM evaluation of Sc and Cu cloud fractions, radiative effects and cloud feedbacks.

Here we leverage the CASCCAD dataset to develop a novel method that separates Sc- from Cu-dominated regimes over tropical oceans. We then use it with the General circulation model-oriented Cloud-Aerosol Lidar and Infrared Pathfinder Satellite Observations (CALIPSO) cloud product (CALIPSO-GOCCP) to evaluate the evolution of tropical Sc and Cu cloud fractions from CMIP5 to CMIP6 ESM generations. Finally, we investigate how changes in ESMs Sc and Cu cloud properties affect low-cloud feedback.

2. Data and methods

2.1. Observations

To evaluate the models in sections 3.1 and 3.2, we use monthly low-cloud fraction (LCF) maps (cloud heights $<$3.36 km) over the tropical oceans, defined as 35°S to 35°N, from CALIPSO-GOCCP observations (Chepfer *et al* 2010), which sample every 333 m along-track near-nadir lidar backscatter profiles for 480 m height intervals. CALIPSO-GOCCP LCF is consistent with the CALIPSO lidar simulator LCF outputs from the models, described in the next section.

To quantify the shortwave cloud radiative effect in the supplementary information (SWCRE, defined as clear-sky minus all-sky fluxes) at the top-of-atmosphere (TOA), we use the monthly mean fluxes from CERES-Energy Balanced and Filled product (CERES-EBAF Ed4.1; Loeb *et al* 2018), which are designed to be compared directly compared with CMIP model outputs.

To select subsidence regimes, we use monthly large-scale pressure vertical wind at 500 hPa ($\omega_{500} > 0$ hPa d^{-1}) from three reanalyses: the 5th generation European Centre for Medium-Range Weather Forecasts atmospheric reanalysis (ERA5, Hersbach *et al* 2020), Modern-Era Retrospective analysis for Research and Applications version 2 (MERRA-2), and National Centers for Environmental Prediction/Department of Energy (NCEP/DOE) reanalysis 2 (Kanamitsu *et al* 2002). Since it is unclear which reanalysis dataset best depicts ω_{500}, we average them together to arguably obtain a best estimate. Using a specific reanalysis dataset instead of the mean does not change qualitatively or quantitatively the results: the associated change in Sc and Cu cloud fractions are smaller than 1% absolute (not shown).

To validate our Sc and Cu discrimination method in section 2.3, we use CASCCAD (Cesana *et al* 2019b), which separates Sc and Cu based on cloud morphology. More specifically, the CASCCAD algorithm identifies overcast Sc, broken Sc, Cu under Sc, Cu with stratiform outflow and isolated Cu using cloud top height, horizontal cloud fraction, vertical cloud fraction variability and horizontal continuity through orbit granules.

All satellite and reanalysis datasets used in this study are monthly means over the 2007–2016 period and over a 2.5° × 2.5° grid.

For cloud feedback estimates (section 3.3), we use the inferred low, Sc and Cu cloud feedbacks from CASCCAD observations over tropical oceans as described in Cesana and Del Genio (2021; see also Supplementary text S1). These feedbacks were computed from the product of CASCCAD-based sensitivities to SST and EIS and potential future SST and EIS pattern changes under an abrupt 4xCO_2 warming scenario and weighted by Sc/(Sc+Cu) fraction. These estimates of cloud feedbacks are in good agreement with other independent observationally inferred estimates (Ceppi and Nowack 2021, Myers *et al* 2021).

2.2. Model simulations

For the model evaluation in sections 3.1 and 3.2, we analyze monthly outputs from global simulations with prescribed SST (following the Atmospheric Model Intercomparison Project, AMIP) from a subset of ten CMIP6 ESMs and their CMIP5 counterparts from the same modeling center, as listed in table 1. We use the last eight years of the CMIP6 simulations (2007–2014) because it partially overlaps with the observational record, and the last eight years of the CMIP5 simulations (2001–2008) to remain consistent. Using the 2001–2008 time period for CMIP6 models does not change qualitatively or quantitatively the results: the changes in multimodel mean

Table 1. We use a subset of 10 CMIP5 and 10 CMIP6 ESMs from the same institutions to best characterize the changes that occurred between CMIP5 and CMIP6 model generations.

Institution	CMIP6	CMIP5
Beijing Climate Centre (BCC)	BCC-CSM2-MR	bcc-csm1–1-m
Canadian Centre for Climate Modelling and Analysis (CCCma)	CanESM5	CanAM4
National Center for Atmospheric Research (NCAR)	CESM2	CCSM4
Centre national de recherches météorologiques (CNRM)	CNRM-CM6-1	CNRM-CM5
Geophysical Fluid Dynamics Laboratory (GFDL)	GFDL-CM4	GFDL-CM3
Goddard Institute for Space Studies (GISS)	GISS-E2-1-G	GISS-E2-R
Met Office Hadley Centre (MOHC)	HadGEM3-GC31-LL	HadGEM2-A
Institut Pierre-Simon Laplace (IPSL)	IPSL-CM6A-LR	IPSL-CM5B-LR
Model for Interdisciplinary Research on Climate (MIROC)	MIROC6	MIROC5
Meteorological Research Institute (MRI)	MRI-ESM2-0	MRI-CGCM3

Sc and Cu cloud fractions are smaller than 0.04% absolute (not shown). We ensure a fair evaluation that accounts for CALIPSO lidar limitations and uses similar cloud definitions as in CALIPSO-GOCCP by utilizing CALIPSO-like model outputs, which explains why we are limited to these ten modeling centers. These outputs were generated using the CALIPSO lidar simulator (Chepfer *et al* 2008) and we further interpolate them on the CALIPSO-GOCCP 2.5° × 2.5° grid. Finally, consistent with the observations, we focus our analysis on subsidence regimes over tropical oceans ($\omega_{500} > 0$ hPa d^{-1}, between 35°S and 35°N), where the high-cloud fraction (cloud heights > 6.72 km) is small and minimally affects the detection of low clouds (see figure S2 of Cesana *et al* 2019a).

In the supplementary information, we compute SWCRE using TOA monthly all-sky (called rsut) and clear-sky (called rsutcs) fluxes, which can be directly compared with CERES-EBAF observations.

In section 3.3, we use cloud feedbacks from Zelinka *et al* (2020), obtained using ESM outputs from the CMIP database in which the atmospheric CO_2 levels were instantaneously quadrupled ($4xCO_2$ experiment) compared to a pre-industrial atmosphere (piControl experiment). The cloud feedback is then computed using the non-cloud radiative kernel method, which quantities the sensitivity of TOA radiation to small perturbations and is adjusted for non-cloud influences (Soden *et al* 2008). In this study, we focus on low-cloud feedbacks, defined as cloud feedbacks from low-level clouds with a cloud-top pressure greater than 680 hPa.

2.3. Sc and Cu discrimination methods

While convective and stratiform clouds are often parameterized separately, distinct low-level convective and stratiform cloud fractions are not typically available in the CMIP5 or CMIP6 archives. As a result, it is particularly difficult to evaluate separately Sc and Cu clouds in widely available climate model output. Perhaps the most straightforward approach to separate Sc- and Cu-dominated gridboxes in an ESM (or any other global dataset) is to define Sc and Cu regimes based on geographical distributions of Sc and Cu using CASCCAD observations. For that purpose, we can identify Sc and Cu regimes using the fraction of Sc clouds, with a metric computed as Sc/(Sc+Cu) in subsidence regime ($\omega_{500} > 0$ hPa d^{-1}), to avoid middle- and high-level cloud overlap, for each month. Here we consider Sc as being all low clouds that are not isolated Cu and therefore the sum of Sc + Cu = LCF. Where Sc/(Sc+Cu) $\geqslant$ 0.5, we define LCFs for Sc and Cu respectively as being LCF_{Sc} = LCF and $LCF_{Cu} = 0$. Conversely, where Sc/(Sc+Cu) < 0.5, $LCF_{Sc} = 0$ and LCF_{Cu} = LCF. However, we note that matching the observations using this geographical method (referred to as Geo method) assumes that ESMs simulate the correct Sc and Cu monthly regimes geographically and necessitates comparing ESM outputs over the same time period as CASCCAD, which is possible for CMIP6 models but not CMIP5.

To address these shortcomings, we have developed another method that can distinguish Sc and Cu monthly cloud regimes in any climate model or observational dataset. This method can be used over any period of time and is independent of environmental variables (e.g., vertical wind, EIS), which have often been used to separate Sc and Cu cloud regimes (e.g., Medeiros and Stevens 2011, Nam *et al* 2012, Myers *et al* 2021) although shortcomings of this traditional method have been noted (Cesana and del Genio 2021, Crnivec *et al* 2023). It is based on the greater area coverage of Sc compared to Cu clouds, that is, their cloud fraction is typically larger than that of Cu over the typical size of an ESM gridbox (~100 km; Cesana *et al* 2019a).

Building on this discriminating characteristic, we separate monthly Sc- and Cu-dominated gridboxes depending on whether their low-cloud fraction is greater or less than the monthly mean LCF over the tropical ocean ($\overline{LCF_{tropics}}$) in subsidence regimes, instead of using the CASCCAD-derived Sc/(Sc+Cu) fraction. For each

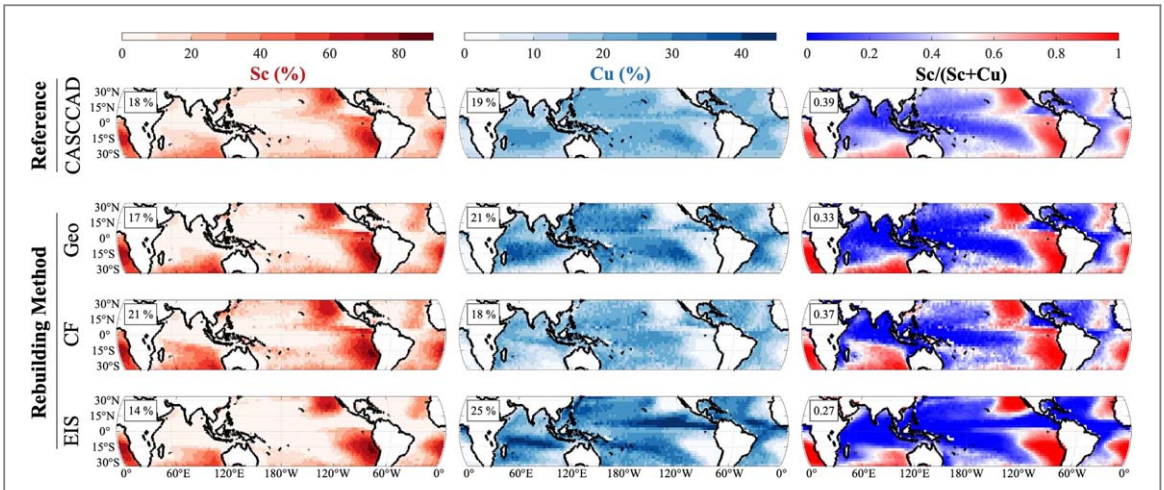

Figure 1. Maps of (left to right) Sc, Cu cloud fractions and Sc/(Cu+Sc) fraction for (top to bottom) CALIPSO-CASCCAD (representing the reference distribution) and CALIPSO-GOCCP v2.9 (2007-2016) using the Geo, CF and EIS methods to separate Sc and Cu clouds (see section 2.3). The means are given in the upper left corner of each map. The linear correlation coefficients between Sc_{geo}, Cu_{geo}, $Sc/(Cu+Sc)_{geo}$ and Sc_{cf}, Cu_{cf}, $Sc/(Cu+Sc)_{cf}$ are 0.94, 0.69 and 0.86.

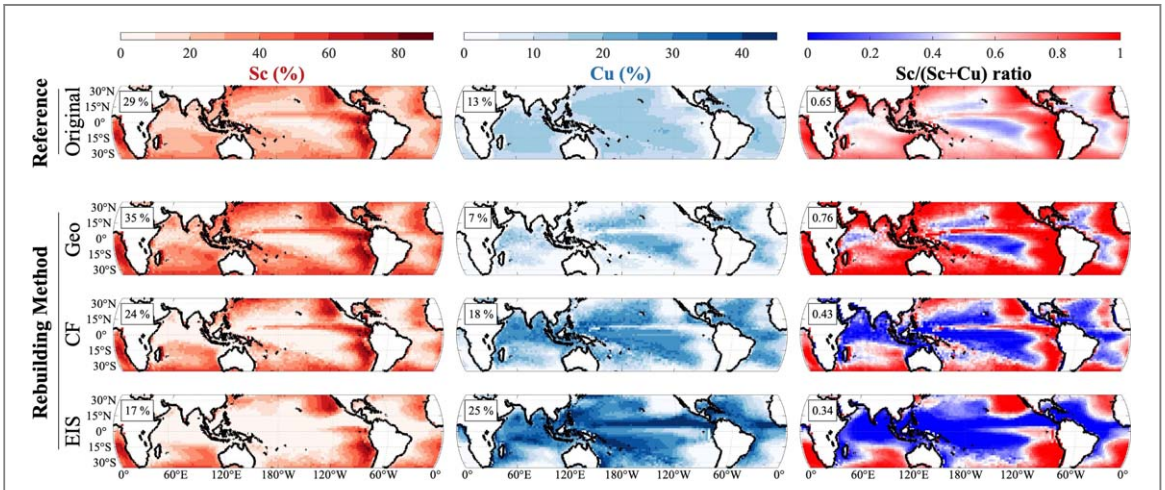

Figure 2. Same as figure 1 but for GISS-ModelE3 model (2007–2014; Cesana *et al* 2021). The linear correlation coefficients between Sc_{geo}, Cu_{geo}, $Sc/(Cu+Sc)_{geo}$ and Sc_{cf}, Cu_{cf}, $Sc/(Cu+Sc)_{cf}$ are 0.95, 0.73 and 0.66.

monthly mean, $LCF_{Sc} = LCF$ and $LCF_{Cu} = 0$ where $LCF \geqslant \overline{LCF_{tropics}}$, and conversely, $LCF_{Sc} = 0$ and $LCF_{Cu} = LCF$ where $LCF < \overline{LCF_{tropics}}$. In the remainder of the study, we present monthly means of these LCF_{Sc} and LCF_{Cu} over the eight-year time period. In addition, we use the same method to define the monthly frequency of occurrence of Sc and Cu cloud regimes in a gridbox for each month, which can correspond to either the Sc or Cu cloud regime, used in figures 5 and 7. Finally, we also compute the Sc and Cu LCF monthly means within their regime, respectively, which we refer to as LCF_{regime}., in figures 5, 6 and 7. This effectively corresponds to averaging LCF where $LCF \geqslant \overline{LCF_{tropics}}$, for $LCF_{Sc,regime}$ and where $LCF < \overline{LCF_{tropics}}$ for $LCF_{Cu,regime}$.

We validate this cloud fraction (CF) method, by comparing the resulting Sc and Cu cloud fractions to those obtained from the CASCCAD-based Geo method, which, by definition, generates Sc- and Cu-dominated cloud fractions the closest to the true CASCCAD Sc and Cu cloud fraction. We find that the Sc- and Cu-dominated cloud fractions from the CF method are highly correlated with that using the Geo method (figure 1), even better than using a threshold based on estimated inversion strength (e.g., EIS = 1 K). The CF method also works very well (and better than the EIS method) with monthly means from the latest version of the GISS-ModelE3 climate model (Cesana *et al* 2021), for which we have access to the constituent Sc and Cu cloud fractions (figure 2). For the sake of simplicity, we refer to these Sc- and Cu-dominated cloud fractions as Sc and Cu cloud fractions in the remainder of the manuscript.

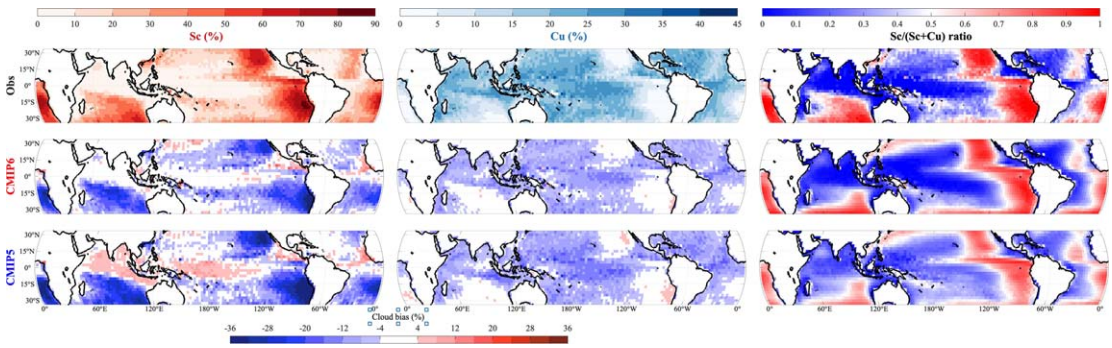

Figure 3. Maps of (left to right) Sc, Cu cloud fractions and Sc/(Cu+Sc) fraction for (top to bottom) CALIPSO-GOCCP v2.9 (2007–2016) and for the CMIP6 and CMIP5 multimodel biases (models minus observations, 2007–2014), using the CF method to separate Sc and Cu clouds (see section 2.3). Note that the CMIP Sc/(Cu+Sc) fractions are actual values and not biases. The linear correlations between observed and simulated Sc, Cu and Sc/(Sc+Cu) ratio are 0.91, 0.82 and 0.88 for the CMIP6 models and 0.87, 0.76 and 0.85 for CMIP5 models, respectively.

3. Results

3.1. Geographical distributions

To evaluate Sc and Cu clouds in CMIP ESMs and their evolution between CMIP5 and CMIP6, we apply the CF method to both CALIPSO-GOCCP observations and the corresponding monthly CMIP simulator outputs from a fixed set of 10 modeling centers across the two CMIP generations (see table 1). Figure 3 shows maps of Sc and Cu cloud fractions—sometimes refer to as cloud covers in the literature—and Sc/(Sc + Cu) fraction for the CALIPSO-GOCCP and the corresponding biases (models minus observations) for CMIP6 and CMIP5 multimodel means. The large Sc decks off the west coasts of continents are well captured in the observations with cloud fractions larger than 90% at the heart of the main decks. By contrast, the Sc cloud fraction is far smaller in the trade wind regions, where Cu clouds dominate and peak at around 30% in some regions. Overall, Sc and Cu clouds appear to be well confined with relatively small overlapping areas, as in CASCCAD observations (figure 1, top row). The CMIP6 multimodel mean reproduces the observed Sc and Cu cloud patterns very well with a notable improvement over that of CMIP5 models, which simulates too much Sc and Cu cloud in Cu- and Sc-dominated regions, respectively, as exemplified by the Sc/(Sc + Cu) fraction (figure 3). However, although collectively, CMIP6 models have substantially increased Sc cloud fraction and slightly increased Cu cloud fraction, both cloud fractions are largely underestimated compared to observations, especially over Sc decks. This issue is investigated into more detail by Crnivec *et al* (2023) with a slightly larger number of models.

We next focus on the zonal distributions of Sc and Cu clouds (figure 4). For this purpose, we not only analyze Sc and Cu cloud fractions (figure 4, top row) but also the frequency of occurrence of each regime (figure 4, middle row) and the cloud fraction mean within each regime (figure 4, bottom row), as described in section 2.3. This decomposition reveals that Sc and Cu cloud fractions within their regimes, and therefore the associated model biases, are rather constant across latitudes in both observations and models, and therefore the variability of CMIP Sc and Cu cloud fraction biases is driven by differences in the frequency of occurrence of Sc and Cu regimes. For example, between 5°S and 15°N, the CMIP Sc cloud fraction bias is very small (figure 4, top row) because the underestimate of the Sc cloud fraction within the Sc regime (figure 4, bottom panel) is compensated by the overestimate of Sc-regime occurrences (figure 4, middle panel). By contrast, between 25°S and 10°S, the CMIP models underestimate both the Sc-regime occurrence and cloud fraction, which results in the largest bias of the Sc cloud fraction across the tropics: an underestimation by a factor of two compared to the observations. On average, the CMIP models overestimate the frequency of occurrence of the Sc regime within the deep tropics (approximately 10°S to 10°N), while they underestimate it elsewhere, and vice versa for the Cu regime. However, here again, our results show that CMIP6 models better depict the observed frequency of Sc and Cu regimes and their associated cloud fractions than their CMIP5 predecessors. Similarly, we find that the overestimate of the shortwave radiative effect –clouds being too bright– has improved in the CMIP6 ensemble but remain large (figure S1). The persistence of the 'too few too bright' problem in CMIP6 models is consistent with a recent study (Konsta *et al* 2022) and is explored in more depth for Sc and Cu regimes by Crnivec *et al* (2023).

3.2. Intermodel variability

While on average, both CMIP6 and CMIP5 ensemble averages fail to reproduce the observed magnitude of Sc and Cu cloud fractions, individual models may do better. For this reason, we explore intermodel tropical means of Sc and Cu cloud fractions, frequencies and regime cloud fractions (figure 5). We find that all ESMs

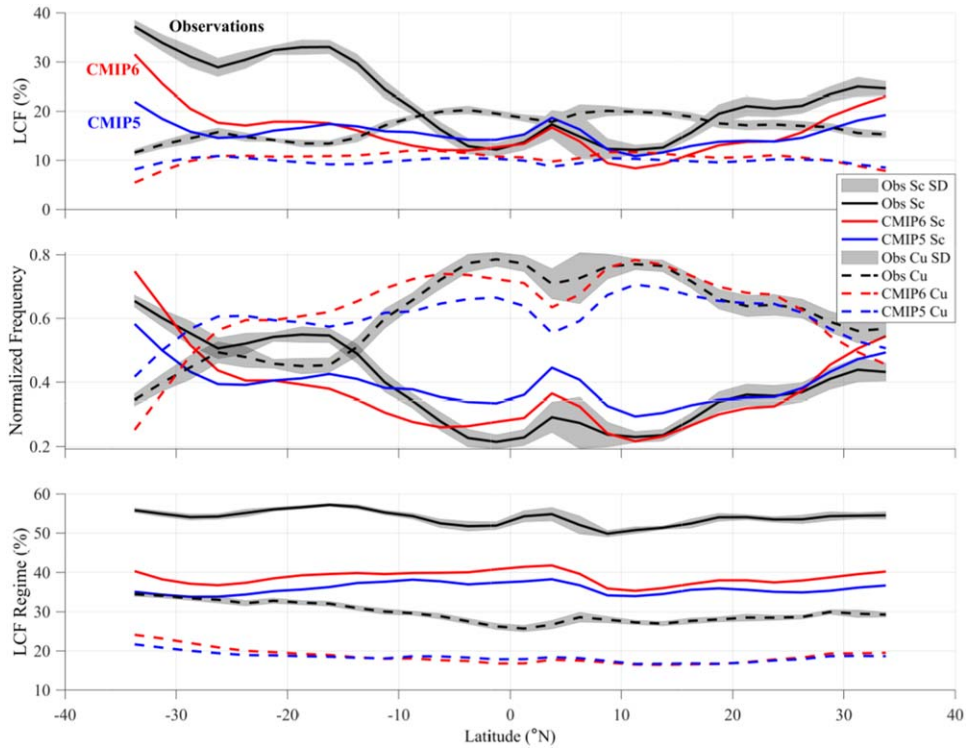

Figure 4. Zonal mean of Sc (solid) and Cu (dashed; top to bottom) cloud fraction means, frequency of regime occurrence and cloud fraction mean within each regime. The black, red and blue lines correspond to the observations, CMIP6 and CMIP5 ESMs, respectively. The shading corresponds to the observed annual standard deviation.

underestimate Cu cloud fraction and all but MIROC5, MIROC6 and IPSL-CM6A underestimate the Sc cloud fraction (figure 5, top panel). Out of these three models, only IPSL-CM6A manages to match the observed Sc frequency and regime mean (figure 5, middle and bottom panels, respectively). The Sc overestimates for MIROC5 and MIROC6 is the result of a large overestimate of the frequency of occurrence of Sc clouds, which more than compensate for the underestimated Sc-regime cloud fraction. On average, CMIP5 ESMs simulate the correct global mean Sc and Cu frequencies (figure 5, middle panel) but the intermodel spread is very large. The CMIP6 ESMs on the other hand slightly underestimate (overestimate) the frequency of Sc (Cu) clouds although their intermodel spread is largely reduced. Furthermore, we note that the zonal variability of Sc and Cu frequencies is better simulated by CMIP6 models (figure 4). In terms of regime mean, CMIP5 and CMIP6 ESMs show a comparable intermodel spread and no specific improvement is noticeable in CMIP6 ESMs beyond a larger multimodel mean for Sc clouds, as reported in the previous section. Finally, it is notable that the ratio of Sc to Cu cloud fraction is overestimated by most models compared to observations—appearing below the black line in figure 5 top panel—with possible implications for cloud feedback given that Sc are more sensitive to warming than Cu (Cesana and Del Genio 2021, Myers *et al* 2021).

3.3. Cloud feedback

In the previous section, we have characterized biases in the representation of Sc and Cu clouds in CMIP ESMs and changes from the CMIP5 to the CMIP6 generation. In this section, we now want to evaluate cloud feedback in Sc- and Cu-dominated regions and explore a possible link between Sc and Cu cloud representation and feedback. For this purpose, we develop a method slightly different from that introduced in section 2.3.

Although observationally inferred Sc and Cu cloud feedbacks are available from CALIPSO-CASCCAD observations (Cesana and Del Genio 2021, Supplementary text S1), there are no equivalent Sc and Cu CMIP-specified model outputs to compare with. As in section 2.3, we design a new method to estimate Sc and Cu feedbacks from the low-cloud feedback and Sc and Cu present-day cloud fractions that can be applied to both observations and simulations for a consistent evaluation. Unlike section 2.3 though, we cannot use the same CF method because it would require monthly mean low-cloud feedbacks, i.e., feedbacks with time dimension, which is missing in the feedbacks we use (Zelinka *et al* 2020).

Instead, we multiply the simulated and observed low-cloud feedback maps by the present-day climatology of either Sc or Cu cloud fraction map with respect to all clouds (i.e., no time dependence) to obtain CF-derived Sc and Cu cloud feedback maps, respectively. By doing so, we implicitly assume that Sc and Cu 2D-geographical

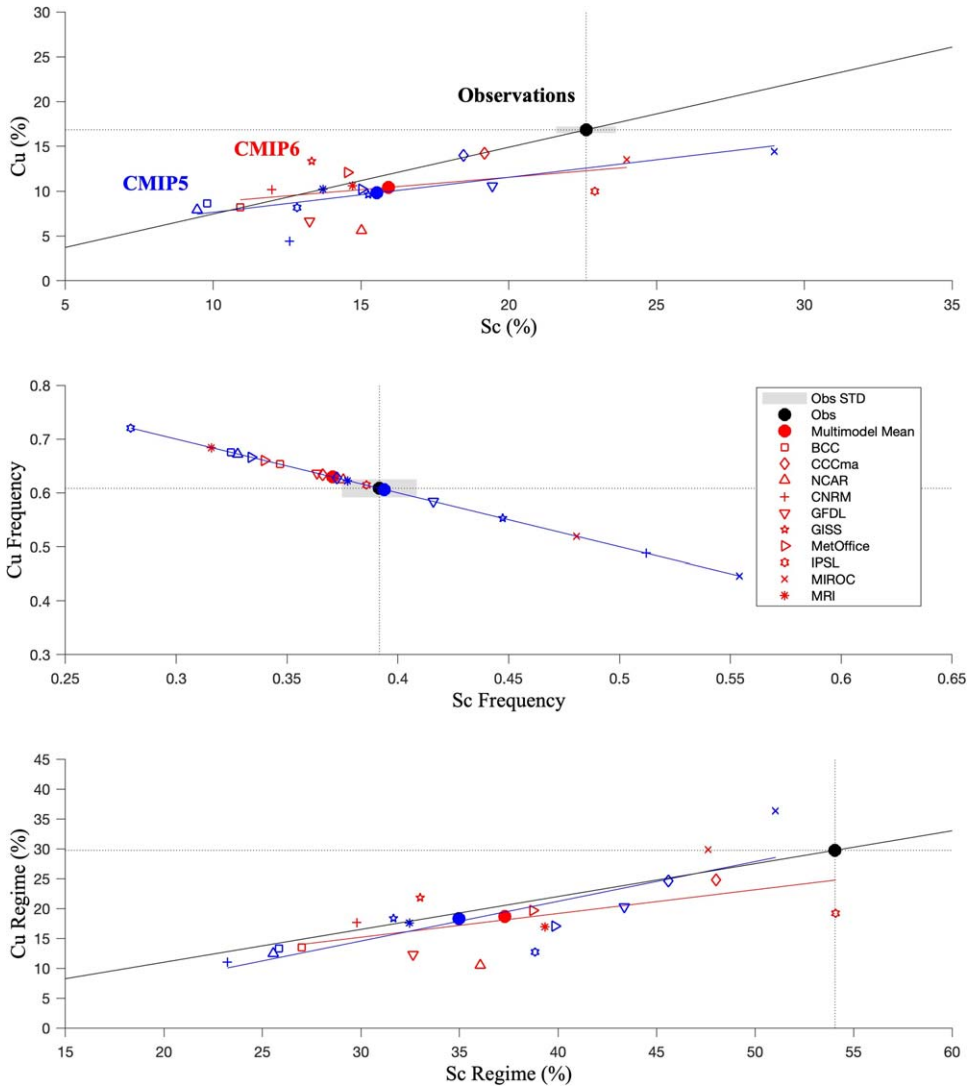

Figure 5. Scatter plot of the tropical mean Sc and Cu (from top to bottom) cloud fraction, frequency of regime occurrence and cloud fraction mean within each regime for the CALIPSO-GOCCP observations (black), the CMIP6 models (red) and the corresponding CMIP5 models (blue). The black lines in the top and bottom panels correspond to the ratio Sc/Cu, meaning that any model below that line favors Sc over Cu clouds compared to observations. The shading corresponds to the observed annual standard deviation.

distributions will remain identical in a warmer climate, which introduces some small uncertainty based on the marginal interannual variability of Sc and Cu clouds (Cesana and Del Genio 2021). This assumption is further supported by results using GISS-ModelE3 (see figure S2), for which using Sc and Cu 2D-geographical distributions from a warmer climate marginally reduces the Sc feedback, and therefore increases Cu feedback, by 0.03 $Wm^{-2}K^{-1}$ (figure S3). Additionally, we use 0.7 $\overline{LCF_{tropics}}$ threshold rather than $\overline{LCF_{tropics}}$, as in section 2.3, to distinguish the Sc and Cu cloud regimes derived from the CF method. Using this smaller threshold in the observations helps increase Sc-dominated and reduce Cu-dominated areas and obtain CF-derived Sc and Cu feedbacks that compare better with our reference CASCCAD-inferred feedbacks, both in terms of mean and pattern correlation (figure 6). Additionally, we note that although using such a threshold respectively increases and decreases Sc and Cu cloud fractions, it does not qualitatively alter the conclusions of our analysis in sections 3.1 and 3.2 (figure S4). On the one hand, we acknowledge that the pattern correlation between the adjusted CF-derived and reference Cu feedbacks and the reference is small, albeit their global means are close. On the other hand, the adjusted CF-method results in a very high pattern correlation and a realistic global mean compared to the reference for the Sc feedback, which drives most of the total low-cloud feedback. Finally, we apply the same method to ESMs to compute Sc- and Cu-dominated feedbacks.

Figure 7 shows tropical maps of Sc and Cu cloud feedback, using the adjusted CF method, for the CASCCAD and CALIPSO-GOCCP observations and the CMIP6 and CMIP5 multimodel means. As in the cloud fraction evaluation, collectively, CMIP6 ESMs substantially improved depiction of Sc cloud feedback both in terms of mean and pattern correlation, as also for Cu clouds to a lesser extent, compared to CMIP5. Yet, we note that both

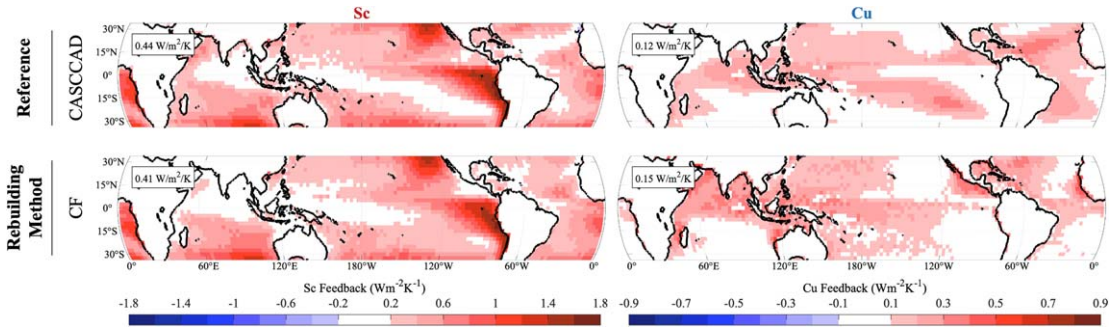

Figure 6. Maps of (left to right) CASCCAD-inferred Sc and Cu (top to bottom) and adjusted CF-derived feedbacks. The means are given in the upper left corner of each map. The linear correlation coefficients between Sc and Cu CASCCAD-inferred feedbacks and Sc_{cf} and Cu_{cf} feedbacks are 0.92 and 0.22, respectively.

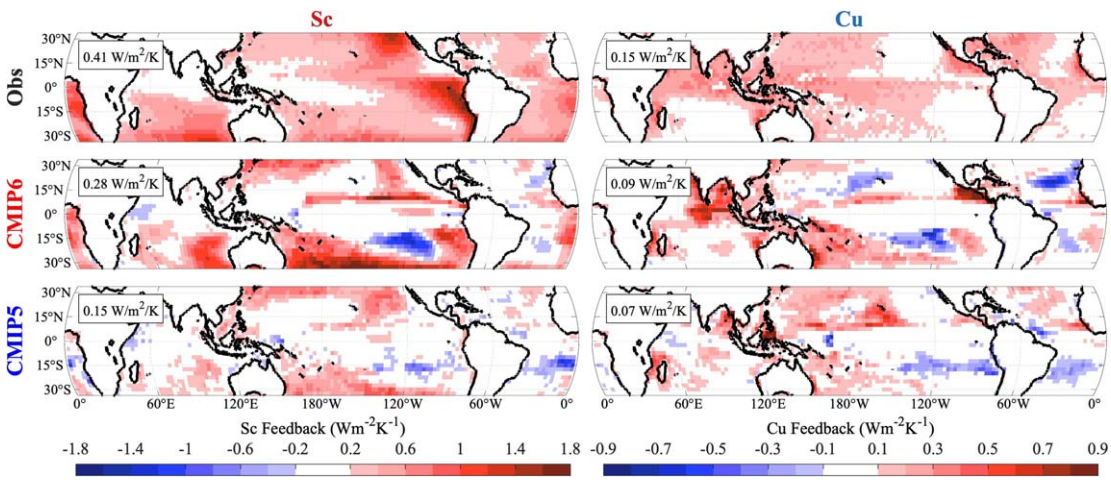

Figure 7. Maps of (left to right) Sc and Cu adjusted CF-derived cloud feedback for (top to bottom) CASCCAD and CALIPSO-GOCCP and for the CMIP6 and CMIP5 models. The means are given in the upper left corner of each map. The linear correlation coefficients between observations and CMIP6 and CMIP5 models are 0.39 and 0.20 for Sc, and 0.30 and 0.22 for Cu, respectively.

generations underestimate the magnitude of the positive feedback. The regions in which the CMIP6 multimodel mean simulates more Sc clouds relative to CMIP5 (the subtropics and in the Peruvian and Namibian decks) loosely correspond to increased Sc positive feedback, implying that the present-day mean state of Sc clouds is at least partly related to how they will evolve in a warmer climate.

We further pursue this hypothesis by showing that the change in low-cloud feedback between CMIP5 and CMIP6 ESMs within the same modeling center correlates well with the change in Sc cloud fraction over Sc-dominated regions, that is in regions where the climatological mean of Sc/(Sc+Cu) fraction over the full period is greater than 0.5 (figure 8). As the Sc cloud fraction in Sc-dominated regions increases between CMIP5 and CMIP6 ESMs, their low-cloud feedback becomes more positive, which partly explains the increase in tropical cloud feedback in the CMIP6 generation (Zelinka *et al* 2020, Cesana and Del Genio 2021). Put simply, the addition of positive-feedback-producing Sc clouds in CMIP6 models naturally resulted in a more positive low-cloud feedback. Even though the correlation ($r = 0.75$) is statistically significant ($p < 0.05$), our sample of models is limited (ten modeling centers). Additionally, we cannot rule out other changes between CMIP5 and 6 model versions contributing to increased low-cloud feedback, which is consistent with the positive intercept of the correlation line between ΔLow feedback and ΔSc (figure 8). On the other hand, we find no significant correlation ($r = 0.24$, $p > 0.05$) between ΔLow feedback and ΔCu (change in Cu cloud fraction within the same modeling center over Cu-dominated regions). Such a result is not surprising since most of the low-cloud feedback is driven by Sc.

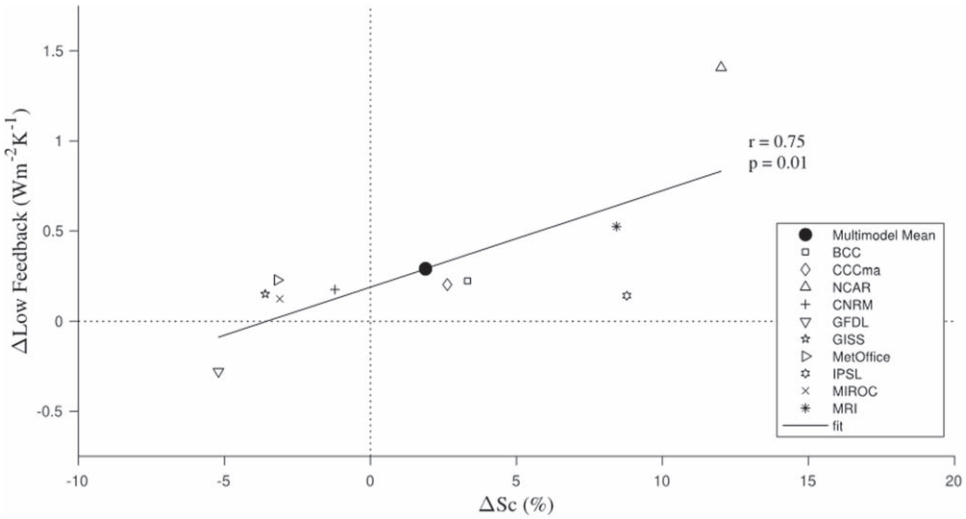

Figure 8. Relationship between the change of Sc-dominated-region cloud fraction and the change low-cloud feedback in CMIP models (CMIP6 minus CMIP5). Linear correlation coefficient (r) is 0.75 and p-value (p) is 0.01.

4. Conclusions and discussions

This study focuses on developing a novel method to distinguish Sc and Cu clouds in observations and climate models based on low-cloud fraction. Our method is independent of traditionally used environmental variables that have limitations. The use of this method together with CALIPSO-GOCCP and CASCCAD satellite observations allows for an evaluation of Sc and Cu clouds and their feedback in the two most recent generations of CMIP ESMs (CMIP6 and CMIP5). Overall, we find that CMIP6 ESMs have collectively improved their depiction of Sc and Cu cloud fractions, cloud radiative effects and cloud feedbacks in terms of pattern and magnitude compared to CMIP5 ESMs, especially that of Sc. However, CMIP6 ESMs continue to underestimate both Sc and Cu cloud fractions and tend to slightly underestimate the frequency of occurrence of Sc—and therefore overestimate that of Cu—on average. The largest CMIP6 Sc cloud biases occur where the models underestimate both the frequency of occurrence of Sc regime and their associated regime cloud fraction (typically south of 10°S), while the smallest biases are identified around the deep tropics (between 5°S and 15°N) where the underestimate of Sc-regime cloud fraction is compensated by an overestimate of the frequency of occurrence of Sc regime. In addition, CMIP6 clouds remain mostly too bright compared to the observations—although better than CMIP5—corresponding to large Sc CRE biases. Using an innovative method and observationally inferred low-cloud feedbacks, we then proceed to show evidence that the multimodel CMIP6 Sc and Cu cloud feedbacks are substantially more realistic than CMIP5's. Finally, our results suggest that part of the increase in the CMIP6 low-cloud feedback (e.g., Zelinka *et al* 2020, Cesana and Del Genio 2021, Myers *et al* 2021) can be traced back to larger Sc cloud fraction in Sc-dominated regions, although our model sample remains limited.

In light of the recent literature (e.g., Cesana and Del Genio 2021, Myers *et al* 2021), Sc feedback seems to be the most important contributor to the tropical low-cloud feedback in contrast with the smaller Cu feedback. Such a difference in Sc and Cu feedback strength helps understand why adding more Sc clouds—that produce a positive feedback—in CMIP6 ESMs has led to greater low-cloud feedback: extending Sc-covered areas cloud fraction therein both serve to amplify their positive feedback. However, the geographical location and magnitude of Sc cloud fraction in the present-day climate are not the only factors at play in determining future Sc cloud feedback; one must also account for the sensitivity of Sc clouds to environmental factors (also known as cloud-controlling factors; (Ceppi and Nowack 2021, Cesana and Del Genio 2021, Scott *et al* 2020, Myers *et al* 2021). The evaluation of Sc and Cu interannual sensitivities to environmental factors using our CF method should help better understand the origins of the large tropical feedback increase in some CMIP6 ESMs, and their subsequent contribution to ECS, which cannot be solely explained by increased Sc cloud fraction magnitude and extent.

Acknowledgments

GC, NC and RP were supported by NOAA grant NA20OAR4310390. GC, AA, and NC were supported by the NASA Modeling, Analysis, and Prediction Program number 80NSSC21K1134. GC and AA were also supported by CloudSat-CALIPSO funding number 80NSSC23K0110. We thank the NASA Center for Climate Simulation (NCCS) at Goddard Space Flight Center for providing computing resources to run the GISS ESM, NASA and CNES for providing access to CALIPSO observations, and Climserv for providing access to CALIPSO-GOCCP observations as well as computing resources. We thank EECLAT and INSU for providing resources to organize a workshop that nurtures discussions between the authors. We also acknowledge the World Climate Research Programme's Working Group on Coupled Modeling, which is responsible for CMIP, and thank the climate modeling groups for producing and making available their model output.

Data availability statement

All data that support the findings of this study are included within the article (and any supplementary files).

Open research

The CALIPSO-GOCCP observations can be downloaded from the CFMIP-Obs website (http://climserv.ipsl.polytechnique.fr/cfmip-obs/Calipso_goccp.html). The CALIPSO-GOCCP CASCCAD statistical datasets can be downloaded from the GISS website (https://data.giss.nasa.gov/clouds/casccad/). CERES-EBAF 4.1 TOA fluxes were downloaded on the CERES website (https://ceres.larc.nasa.gov/data/#ebaftoa-level-3). Three reanalysis datasets were used in the study for temperatures: the 5th generation European Centre for Medium-Range Weather Forecasts atmospheric reanalysis (ERA5, downloaded from https://doi.org/10.24381/cds.6860a573 and by selecting monthly averaged reanalysis and the temperature variable, the Modern-Era Retrospective analysis for Research and Applications version 2, downloaded from https://disc.gsfc.nasa.gov/datasets/M2IMNPASM_5.12.4/summary (https://doi.org/10.5067/2E096JV59PK7), and *National Centers for Environmental Prediction / Department of Energy* (NCEP/DOE) reanalysis 2, downloaded from http://www.cpc.ncep.noaa.gov/products/wesley/reanalysis2/.

The CMIP ESM outputs used in this study—listed in table 1-were downloaded from the ESGF (https://esgf-node.llnl.gov/) and the feedbacks from Zelinka *et al* (2020) at 10.5281/zenodo.5206851.

ORCID iDs

G V Cesana https://orcid.org/0000-0002-8899-0509
R Pincus https://orcid.org/0000-0002-0016-3470

References

Andrews T, Gregory J M, Webb M J and Taylor K E 2012 Forcing, feedbacks and climate sensitivity in CMIP5 coupled atmosphere-ocean climate models *Geophys. Res. Lett.* **39** 1–7

Andrews T and Webb M J 2018 The dependence of global cloud and lapse rate feedbacks on the spatial structure of tropical pacific warming *J. Clim.* **31** 641–54

Bony S and Dufresne J L 2005 Marine boundary layer clouds at the heart of tropical cloud feedback uncertainties in climate models *Geophys. Res. Lett.* **32** L20806

Caldwell P M, Zelinka M D, Taylor K E and Marvel K 2016 Quantifying the sources of intermodel spread in equilibrium climate sensitivity *J. Clim.* **29** 513–24

Ceppi P and Nowack P 2021 Observational evidence that cloud feedback amplifies global warming *Proc. Natl Acad. Sci.* **118** 2026290118

Cesana G, Del Genio A D, Ackerman A S, Kelley M, Elsaesser G, Fridlind A M, Cheng Y and Yao M-S 2019a Evaluating models' response of tropical low clouds to SST forcings using CALIPSO observations *Atmos. Chem. Phys.* **19** 2813–32

Cesana G, del Genio A D and Chepfer H 2019b The cumulus and stratocumulus cloudsat-CALIPSO dataset (CASCCAD) *Earth System Science Data Discussions* **2667637** 1–33

Cesana G v, Ackerman A S, Fridlind A M, Silber I and Kelley M 2021 Snow reconciles observed and simulated phase partitioning and increases cloud feedback *Geophys. Res. Lett.* **48** 1–11

Cesana G v and del Genio A D 2021 Observational constraint on cloud feedbacks suggests moderate climate sensitivity *Nat Clim Chang* **11** 213–8

Chepfer H, Bony S, Winker D, Cesana G, Dufresne J L, Minnis P, Stubenrauch C J and Zeng S 2010 The GCM-oriented CALIPSO cloud product (CALIPSO-GOCCP) *J. Geophys. Res.* **115** D00H16

Chepfer H, Bony S, Winker D, Chiriaco M, Dufresne J-L and Sèze G 2008 Use of CALIPSO lidar observations to evaluate the cloudiness simulated by a climate model *Geophys. Res. Lett.* **35** L15704

Crnivec N, Cesana G and Pincus R 2023 Evaluating the representation of tropical stratocumulus and shallow cumulus clouds as well as their radiative effects in CMIP6 models using satellite observations Online: (10.22541/essoar.167336758.80322023/v1)

Hersbach H *et al* 2020 The ERA5 global reanalysis *Q. J. R. Meteorolog. Soc.* **146** 1999–2049
Kanamitsu M, Ebisuzaki W, Woollen J, Yang S-K, Hnilo J J, Fiorino M and Potter G L 2002 NCEP-DOE AMIP-II Renalalysys (R-2) *Bull. Am. Meteorol. Soc.* **83** 1631–43
Klein S A, Hall A, Norris J R and Pincus R 2017 Low-Cloud Feedbacks from Cloud-Controlling Factors: A Review *Surv Geophys* **38** 1307–29
Konsta D, Dufresne J L, Chepfer H, Vial J, Koshiro T, Kawai H, Bodas-Salcedo A, Roehrig R, Watanabe M and Ogura T 2022 Low-level marine tropical clouds in six CMIP6 models are too few, too bright but also too compact and too homogeneous *Geophys. Res. Lett.* **49** e2021GL097593
Loeb N G, Doelling D R, Wang H, Su W, Nguyen C, Corbett J G, Liang L, Mitrescu C, Rose F G and Kato S 2018 Clouds and the earth's radiant energy system (CERES) energy balanced and filled (EBAF) top-of-atmosphere (TOA) edition-4.0 data product *J. Clim.* **31** 895–918
Medeiros B and Stevens B 2011 Revealing differences in GCM representations of low clouds *Clim. Dyn.* **36** 385–99
Myers T A, Scott R C, Zelinka M D, Klein S A, Norris J R and Caldwell P M 2021 Observational constraints on low cloud feedback reduce uncertainty of climate sensitivity *Nat Clim Chang* **11** 501–7
Nam C, Bony S, Dufresne J and Chepfer H 2012 *The 'Too Few, Too Bright' Tropical Low-Cloud Problem In Cmip5 Models* **39** 1–7
Rémillard J, Kollias P, Luke E and Wood R 2012 Marine boundary layer cloud observations in the Azores *J. Clim.* **25** 7381–98
Scott R C, Myers T A, Norris J R, Zelinka M D, Klein S A, Sun M and Doelling D R 2020 Observed sensitivity of low-cloud radiative effects to meteorological perturbations over the global oceans *J. Clim.* **33** 7717–34
Soden B J and Held I M 2006 An assessment of climate feedbacks in coupled ocean–atmosphere models *J. Clim.* **19** 3354–60
Soden B J, Held I M, Colman R C, Shell K M, Kiehl J T and Shields C A 2008 Quantifying climate feedbacks using radiative kernels *J. Clim.* **21** 3504–20
Qu K, Hall A, Klein S A and Deangelis A M 2015 Positive tropical marine low-cloud cover feedback inferred from cloud-controlling factors *Geophys Res Lett* **42** 7767–75
Vial J, Dufresne J L and Bony S 2013 On the interpretation of inter-model spread in CMIP5 climate sensitivity estimates *Clim. Dyn.* **41** 3339–62
Zelinka M D, Klein S A, Taylor K E, Andrews T, Webb M J, Gregory J M and Forster P M 2013 Contributions of different cloud types to feedbacks and rapid adjustments in CMIP5 *J. Clim.* **26** 5007–27
Zelinka M D, Myers T A, McCoy D T, Po-Chedley S, Caldwell P M, Ceppi P, Klein S A and Taylor K E 2020 Causes of higher climate sensitivity in CMIP6 models *Geophys. Res. Lett.* **47** 1–12
Zelinka M D, Zhou C and Klein S A 2016 Insights from a refined decomposition of cloud feedbacks *Geophys. Res. Lett.* **43** 9259–69